Supporting Information

Kim et al. 10.1073/pnas.1406926111

SI Theoretical Calculation Details

Lattice Constant Matching. The molecular junctions we considered are Au/molecule/graphite junctions with Au(111) layers and graphite (0001) layers. We use a 5×5 supercell for the Au(111) surface with an Au-Au bond length of 2.960 Å in contrast to the experimental bond length of 2.865 Å and the Perdew-Burke-Ernzerhof (PBE) Au-Au bond length of 2.984 Å. We use a 6×6 supercell for the graphite (0001) surface, with a PBE C-C bond length of 1.424 Å in contrast to the experimental bond length of 1.421 Å. We use an inter-layer distance (c) of 3.354 Å for graphite which is the same as the experimental value but smaller than the PBE value by 20%. This results in a hexagonal supercell lattice with a = 14.80 Å.

Geometry Optimization and Binding Energy Calculation. We optimize geometry of benzenediamine (BDA) and terphenyldiamine (TBDA) on a graphite (0001) surface and calculate binding energies using van der Waals (vdW)–DF2 (1) functional with the Vienna ab initio simulation package (2), using projector augmented wave potential (3) and a 400-eV plane-wave cutoff. For geometry optimization, 4×4 graphite supercell with four layers and $2 \times 2 \times 1$ k-mesh are used for BDA (6×6 supercell is used for TBDA). Positions of all carbon atoms in graphite are fixed. Twelve different structures are obtained, with different angle θ between molecular backbone and graphite surface, as discussed in the main text. For binding energy calculation of each structure, 6×6 supercell with two layers and $3 \times 3 \times 1$ k-mesh are used. We check convergence using four layers and $6 \times 6 \times 1$ k-mesh.

Transmission Calculation of Junctions. We form Au/BDA/graphite junctions with seven layers of Au (111) and six layers of graphite (0001). The last graphite layer and the last gold layer serve as "buffer atoms" needed for transmission calculation with dissimilar electrodes. Three layers of gold and two layers of graphite serve as the left and right electrodes, respectively (4). A gold adatom on Au (111) surface is placed 2.5 Å directly above the upper nitrogen of BDA molecule. This has been shown in previous work to model the experimental setup very well. All gold atoms and carbon atoms in graphite are also fixed in bulk values as described in *Lattice Constant Matching*.

Overall, 12 molecular junctions are formed, with different angles θ. We use PBE functional (5) and double-zeta polarization basis sets for all elements except Au, for which we use a specially tuned pseudopotential and single-zeta polarization basis that is used previously (6). Here, 6×6 Γ-centered k-mesh is used for self-consistent calculation of the density matrix and Hamiltonian, and 36×36 k-mesh (shifted off Γ by half of a reciprocal lattice spacing) is used for non-self-consistent transmission calculation. To produce smooth and accurate density of states near Fermi level for graphite electrode, we add a 0.005-eV imaginary part to the energy grid in the calculation of Green's function, which effectively generates broadening. Special attention is paid to the numerical stability of the calculation for very low transmission.

To account for PBE's underestimation of level alignment between junction Fermi level and highest occupied molecular orbit of the molecule, we apply a self-energy correction to the molecular subspace, which includes two contributions (6, 7): (*i*) gas phase correction. We use 2.6 eV for benzenediamine and 2.1 eV for terphenyldiamine, consistent with previous work (8); and (*ii*) surface polarization effect, which is approximated by a (classical) image charge interaction between Mulliken charge of the gas phase molecule and its images. We use an image plane 1.47 Å above Au (111) surface and another image plane 1.0 Å above graphite (0001) surface.

Junction Polarization Effect. In the experimental measurement, a bias voltage 0.5 V is used. In our integration of transmission curve, *T(E)* is from a zero-bias calculation. This approach neglects the polarization effect of the junction, which is a response of the molecule to the external bias and results in *T(E)* from finite-bias calculation slightly different from zero-bias *T(E)*. However, from the work of Darancet et al. (9), we know that at small biases, *T(E)* is roughly a rigid shift of zero-bias *T(E)*. Due to the high computational cost of finite-bias calculation, in this work, we calculate *T(E)* under 0.1-V bias, and the bias induced effects at 0.5 V using an extrapolation.

In Fig. S5, we show the *T(E)* from zero-bias calculation (red) and that from a 0.1-V bias (blue) on the graphite, using the 3° geometry of BDA. The 0.1-bias *T(E)* is shifted by ∼0.04 eV upward. This is further confirmed by the current calculated from a 0.1-V finite-bias calculation and the integration of zero-bias *T(E)* over −0.04 to +0.06 eV region. The former yields 1.259×10^{-10} A, and the latter yields 1.261×10^{-10} Å, which are very close.

Under a 0.5-V bias, we assume *T(E)* shifts by 0.2 eV upward. Therefore, we integrate *T(E)* from −0.2 to +0.3 V or −0.3V to +0.2V and divide the results by 0.5 V to determine the conductance and rectification to compare with experiments.

Integration of Transmission Curve. In the experiments, the conductance is measured under a −0.5-V bias applied to the substrate. To compare calculations to experiments, we determine the current using the Landauer formula (10) using a zero temperature limit, and divide the current by the bias to get conductance as:

$$G = \frac{\frac{2e^2}{h}\int_{\mu_L}^{\mu_R} T(E)dE}{\mu_R - \mu_L}.$$

Here, G is conductance; μ_L and μ_R are the chemical potentials at left electrode and right electrode, respectively; *T(E)* is the calculated transmission; and $2e^2/h$ is conductance quantum. In the case of Au/BDA/graphite junction, a −0.5-V bias is applied to the graphite electrode, which means graphite chemical potential is 0.5 eV higher than the gold chemical potential (Fig. 4*B*). We therefore integrate *T(E)* over a 0.5-eV range between E_F −0.2 eV to E_F + 0.3 eV, where E_F is Fermi level; i.e., we set $\mu_L = -0.2$ and $\mu_R = +0.3$ V in the equation above. Conductance calculated from this method agrees well with experimental measurement, and zero-bias conductance calculated in the usual way; i.e., *T(E = 0)* that corresponds to $\mu_L = \mu_R$, greatly underestimate conductance. Fig. S6 shows the comparison between calculated conductance using the above method and the zero-bias conductance *T(E = 0)*.

1. Lee K, Murray ÉD, Kong L, Lundqvist BI, Langreth DC (2010) Higher-accuracy van der Waals density functional. *Phys Rev B* 82(8):081101.
2. Kresse G, Furthmüller J (1996) Efficient iterative schemes for *ab initio* total-energy calculations using a plane-wave basis set. *Phys Rev B Condens Matter* 54(16):11169–11186.
3. Blöchl PE (1994) Projector augmented-wave method. *Phys Rev B* 50(24):17953–17979.

4. Brandbyge M, Mozos JL, Ordejon P, Taylor J, Stokbro K (2002) Density-functional method for nonequilibrium electron transport. *Phys Rev B* 65(16):165401.
5. Perdew JP, Burke K, Ernzerhof M (1996) Generalized gradient approximation made simple. *Phys Rev Lett* 77(18):3865–3868.
6. Quek SY, et al. (2007) Amine-gold linked single-molecule circuits: Experiment and theory. *Nano Lett* 7(11):3477–3482.
7. Neaton JB, Hybertsen MS, Louie SG (2006) Renormalization of molecular electronic levels at metal-molecule interfaces. *Phys Rev Lett* 97(21):216405.
8. Quek SY, Choi HJ, Louie SG, Neaton JB (2009) Length dependence of conductance in aromatic single-molecule junctions. *Nano Lett* 9(11):3949–3953.
9. Darancet P, Widawsky JR, Choi HJ, Venkataraman L, Neaton JB (2012) Quantitative current-voltage characteristics in molecular junctions from first principles. *Nano Lett* 12(12):6250–6254.
10. Büttiker M, Imry Y, Landauer R, Pinhas S (1985) Generalized many-channel conduc tance formula with application to small rings. *Phys Rev B Condens Matter* 31(10): 6207–6215.

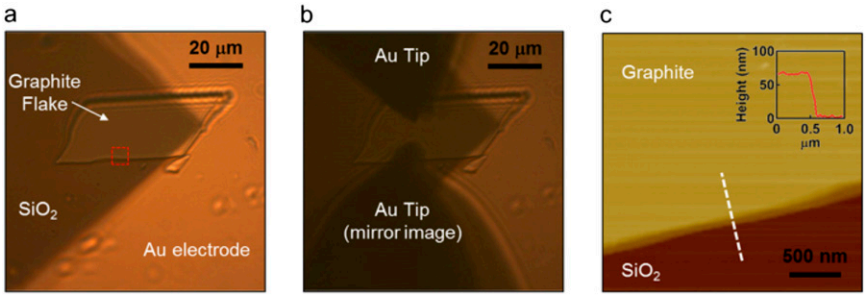

Fig. S1. (*A*) Optical microscope image of Au electrode deposited on the graphite flake using a shadow mask method. (*B*) Optical microscope image of Au tip approaching the graphite surface. (*C*) Atomic force microscope topography image and the height profile (*Inset*) for the edge of the graphite flake in the red box in *A*.

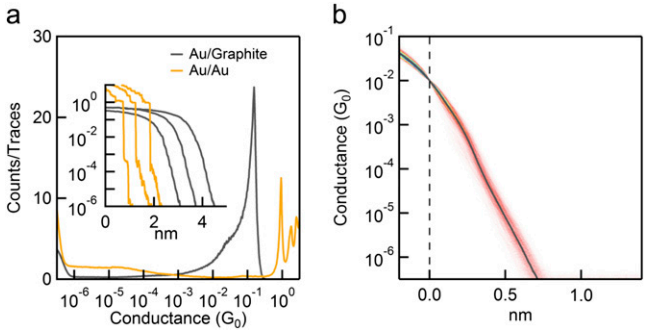

Fig. S2. (*A*) Normalized 1D conductance histogram for the measurement in the absent of molecule with Au/Au (yellow) and Au/graphite (gray) electrodes. (*Inset*) Sample conductance traces for measurements without molecules made with Au/Au (yellow) and Au/graphite (gray) electrodes. (*B*) Normalized 2D conductance histogram and the line profile (gray) for the measurements without molecules made with Au/graphite electrode.

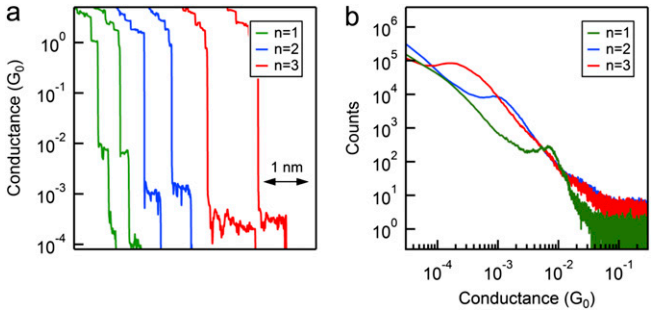

Fig. S3. (*A*) Sample conductance traces for the measurement in the presence of molecules made by first dipping an Au tip wire in a 1,2,4-trichlorobenzene molecular solution, drying the tip under N_2 before the measurements on an Au substrate electrode. (*B*) The 1D conductance histogram of measurements using a molecule-coated Au tip and Au substrate with BDA (green), biphenyldiamine (DBDA; blue), and TBDA (red).

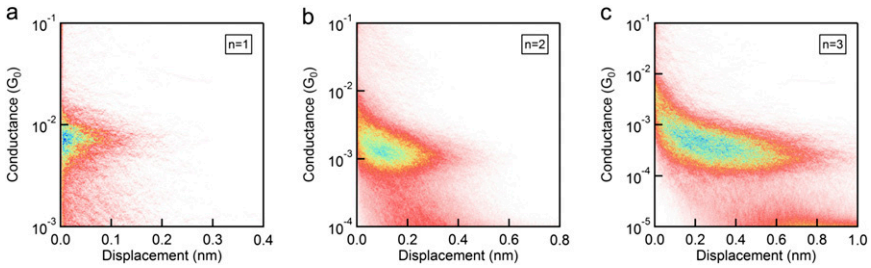

Fig. S4. Normalized 2D histogram for BDA (*A*), DBDA (*B*), and TBDA (*C*) measured with Au electrodes.

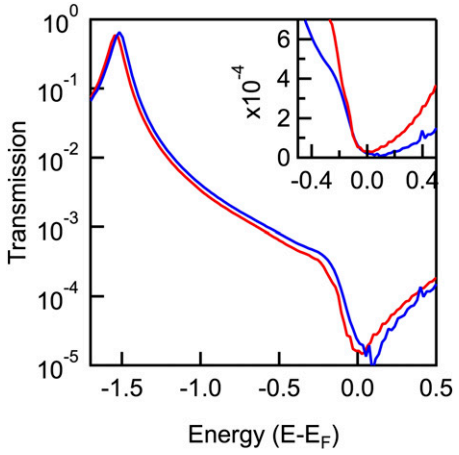

Fig. S5. Transmission function *T(E)* for 3° geometry of graphite/BDA/Au junction at zero bias (red) and 0.1 V (blue). *Inset* shows the same curves around E_F.

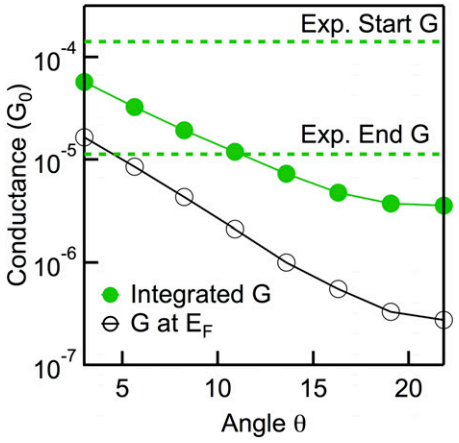

Fig. S6. Comparison of conductance calculated by integrating the transmission curve between −0.2 and 0.3 eV (green circles), zero-bias conductance (black circles), and experimental values (dashed lines as shown in Fig. 3*C*).

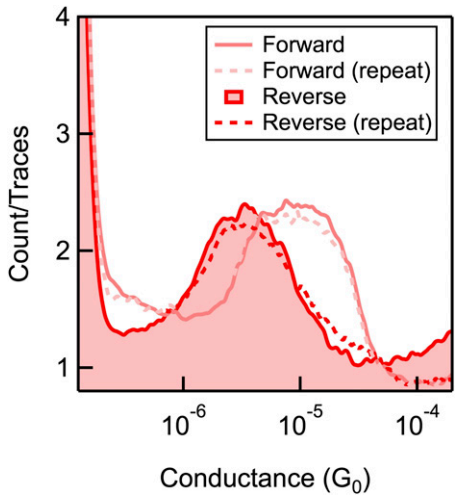

Fig. S7. Histograms created from conductance traces measured with TBDA while applying a negative (dark red, reverse bias) and positive (light red, forward bias) bias to the graphite substrate measured on two different samples (solid and dashed lines) to show reproducibility of the data.

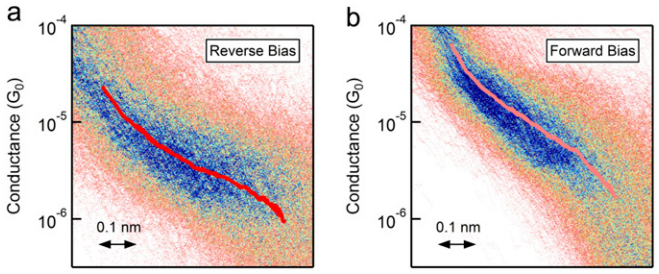

Fig. S8. Normalized 2D histogram for graphite/TBDA/Au junctions measured with (*A*) a reverse bias of −0.5 V applied to the graphite and (*B*) a forward bias of 0.5 V applied to the graphite electrode.